MitoTALEN reduces mutant mtDNA load and restores tRNA[Ala] levels in a mouse model of heteroplasmic mtDNA mutation

Sandra R. Bacman[1,*], **Johanna H. K. Kauppila**[2], **Claudia V. Pereira**[1], **Nadee Nissanka**[1], **Maria Miranda**[2], **Milena Pinto**[1], **Sion L. Williams**[1], **Nils-Göran Larsson**[2], **James B. Stewart**[2], **Carlos T. Moraes**[1,*]

[1]Department of Neurology, University of Miami Miller School of Medicine, Miami, USA.

[2]Department of Mitochondrial Biology, Max Planck Institute for Biology and Ageing, Cologne, Germany.

Abstract

Mutations in the mitochondrial DNA (mtDNA) are responsible for several metabolic disorders, commonly involving muscle and the central nervous system[1]. Because of the critical role of mtDNA in oxidative phosphorylation, the majority of pathogenic mtDNA mutations are heteroplasmic, co-existing with wild-type molecules[1]. Using a mouse model with a heteroplasmic mtDNA mutation[2], we tested whether mitochondrial-targeted TALENs (mitoTALENs)[3,4] could reduce the mutant mtDNA load in muscle and heart. AAV9-mitoTALEN was administered via intramuscular, intravenous, and intraperitoneal injections. Muscle and heart were efficiently transduced and showed a robust reduction in mutant mtDNA, which was stable over time. The molecular defect, namely a decrease in transfer RNA[Ala] levels, was restored by the treatment. These results showed that mitoTALENs, when expressed in affected tissues, could revert disease-related phenotypes in mice.

Mitochondrial disorders are a heterogeneous group of genetic diseases that affect the mitochondrial oxidative phosphorylation (OXPHOS) system. Inheritance can be Mendelian when mutations are in nuclear genes, or maternal when mutations are in the mtDNA. In

either case, high-energy-demand tissues such as skeletal muscle and brain are usually affected. In humans with mitochondrial diseases mutant mtDNA commonly co-exists with wild-type (WT) mtDNA, resulting in mtDNA heteroplasmy. The level of mutant and WT mtDNAs are key to the development and severity of clinical phenotypes. Gene editing tools have been used to selectively reduce the relative levels of mutant mtDNA in cultured cells[3–5]. Key to these approaches is the ability of cells to maintain a stable mtDNA copy number, which allows for residual mtDNA to repopulate the organelle network.

Mouse models with heteroplasmic pathogenic mtDNA mutations were not available until recently, when a mouse with a heteroplasmic mitochondrial tRNA[Ala] gene mutation was generated[2]. This mtDNA mutation, m.5024C>T was associated with tRNA[Ala] instability and a mild cardiac phenotype at older ages. The mouse mutation resembles human mtDNA mutations in tRNA[Ala], which were associated with myopathies and OXPHOS deficiencies[6]. In the present study we show that mitoTALENs can efficiently reduce the mutant mtDNA load in skeletal muscle and heart, restoring the levels of mitochondrial tRNA[Ala].

To test whether mitoTALENs can alter mtDNA heteroplasmy in vivo, we developed TALENs specific for the mouse mtDNA region harboring the m.5024C>T mutation (Fig. 1a,b). TALENs work as dimers and we designed one of the monomers to preferentially recognize the mutant sequence. We took advantage of the required "T" at position zero of the TALEN architecture[7] to target the mutant m.5024C>T allele (Fig. 1a). The DNA sequence of each TALEN monomer was cloned downstream of a mitochondrial localization signal and an epitope tag (Fig. 1b). Monomer A binds to the m.5024C>T and contains 9.5 repeat variable diresidues (RVDs). Monomer B, which binds to the adjacent WT mtDNA sequence, contained 15.5 RVDs. Heterodimeric *Fok*I nuclease domains were used to reduce homodimer-driven off-site cleavage[8,9]. In addition, fluorescent markers (mCherry or eGFP), which were separated from the mitoTALEN coding region by a T2A picornavirus ribosome stuttering sequence[3,10], were added. Mitochondrial localization was verified by immunocytochemistry (Fig. 1c,d, left panels and Supplementary Fig. 1a). The presence of full-length mitoTALEN monomers A and B was confirmed by western blots (Fig. 1c,d right panels and Supplementary Fig. 1b,d). To facilitate viral packaging we also used a shortened version of monomer B, with only 8.5 RVDs (monomer C) (Fig. 1a,b). Expression and mitochondrial localization was also confirmed for monomer C (Supplementary Fig. 1b–d).

To test the efficacy of the mitoTALENs, we transfected mouse embryonic fibroblasts (MEFs) derived from heteroplasmic mice carrying the m.5024C>T mutation with both plasmids coding mitoTALEN monomers (A and B). One day after transfection, cells were FACS sorted. Cell populations expressing both eGFP and mCherry were termed "Yellow," and cells sorted as negative for the markers were termed "Black." There were significant changes in mtDNA heteroplasmy, with a decrease in the mutant genotype in the "Yellow" cell population (Fig. 1e,f). Similar results were obtained with monomers A and C (Fig. 1e,g). There were no significant changes in total mtDNA levels after 24 hours (Fig. 1h). The specificity of the mitoTALENs was also evaluated by transfecting C57BL/6J fibroblasts containing only the WT m.5024C allele. No significant mtDNA depletion was observed in these cells after treatment (Supplementary Fig. 1e).

To better observe a change in phenotype we developed MEF clones with higher levels of mutant mtDNA. A MEF clone carrying higher levels of mutation m.5024C>T (Clone 5, 85% mutant mtDNA) was obtained as described in the Methods. This clone with higher mutant levels was transfected for 24 h with the mitoTALEN against the m.5024C>T allele (monomers A and B). Again, a robust change in heteroplasmy was observed as soon as one day after transfection, which persisted at 3 weeks (Supplementary Fig. 1f,g). The "Black" cell population showed a small shift in heteroplasmy, which became more evident with time in culture (Supplementary Fig. 1g). When examined under the microscope two days after sorting, we observed a few fluorescent cells in the "Black" population, explaining those small changes. Significant changes in the total mtDNA levels were not detected in "Yellow" cells (Supplementary Fig. 1h). Two mitochondrial proteins know to be unstable in cells with high levels of mutant mtDNA (NDUFB8 and COXI)[4] were found to be increased in the "Yellow" cells 2 weeks after transfection with the mitoTALENs (Supplementary Fig. 1i).

MitoTALEN monomers A and C (C was used instead of B because of its smaller size) were cloned in AAV9 vectors to produce viral particles that could be used in in vivo experiments. Viral particles derived from each mitoTALEN monomer were injected together in the right tibialis anterior muscle of mice carrying the heteroplasmic m.5024C>T mutation. Toe biopsies showed that heteroplasmy levels varied between animals. The left leg tibialis anterior was injected with control AAV9-GFP. To evaluate the expression of mitoTALEN monomers, western blots for the HA- and FLAG-tags, and GFP were analyzed 4 weeks after injection (Fig. 2a,b). Expression was also observed after 10 weeks (Supplementary Fig. 2a). Immunohistochemistry analysis showed widespread homogeneous expression of the T2A-driven GFP from the AAV9-mitoTALEN in the injected tibialis anterior (Fig. 2c). Likewise, the AAV9-GFP injected left tibialis anterior showed widespread GFP expression (Supplementary Fig. 2b). Restriction-fragment length polymorphism (RFLP) analyses showed a strong decrease in mutant/WT mtDNA ratios in the right tibialis anterior (injected with AAV9-mitoTALEN) when compared to the left tibialis anterior (injected with the control AAV9-GfP) (Fig. 2d,e). The shift in heteroplasmy was observed after a single intramuscular injection in all analyzed mice. This was true for samples obtained at 4, 6, 10, 12, and 24 weeks after injection (Fig. 2d,e). When percentage mutant mtDNA change was analyzed per "time after injection" group, significance was obtained starting at 6 weeks (Fig. 2f). However, statistical power was greatly reduced because of the different mutant levels among mice. Tissues adjacent to the tibialis anterior, such as quadriceps and gastrocnemius, which were not directly injected, also showed a reduction in mutant mtDNA in a few mice. However, in contrast to the injected TAs, this was not seen in all animals, suggesting that injection variations can allow for neighboring muscles to be transduced, probably by intersticial diffusion (Supplementary Fig. 2c,d).

We did not detect decreased levels of total mtDNA in the tibialis anterior after 6, 12, or 24 weeks when compared to the left control-injected TAs, suggesting that the degradation of mutant mtDNA was compensated for by mtDNA replication (Supplementary Fig. 2e).

The molecular pathology in the m.5024C>T mouse is caused by the destabilization of mutant tRNA[Ala] and the consequent reduction in its steady-state levels, which was shown in heart[2]. We found the same molecular pathology in skeletal muscle, with no change in any

other mitochondrial transcript analyzed (Supplementary Fig. 3a,b). We found that there was a decrease in tRNA^{Ala} levels in skeletal muscle when the mutation load was higher than 50% (Supplementary Fig. 3c). Therefore, we analyzed the injected muscles for a possible recovery of this molecular phenotype. The levels of mitochondrial tRNA^{Ala} were expressed as ratios to the mitochondrial tRNA^{Trp}. A recovery of tRNA^{Ala} levels (Fig. 2g–j) was observed in the right tibialis anterior of mice harboring high levels of mutant mtDNA (Fig. 2k,l), as only these samples had decreased tRNA^{Ala} levels to start with (Fig. 2g–j).

We also tested whether systemic administration of mitoTALEN could alter mtDNA heteroplasmy in muscle. Retro-orbital injection, which rapidly drains into the venous system, has been proven to be an efficient delivery method for recombinant AAV, especially in young mice[11]. We injected 15–17-day-old mice heteroplasmic for the tRNA^{Ala} mutation and evaluated different tissues targeted by the recombinant AAV9 serotype at 6 and 12 weeks post-injection. Positive FLAG and HA expression was observed in heart, gastrocnemius, quadriceps, and tibialis anterior muscles (Fig. 3a). No expression was observed in kidney or brain. Likewise, GFP expression was observed in all skeletal and cardiac tissues analyzed, but not in kidney or brain after injection of the AAV9-mitoTALEN, which also expresses GFP (Fig. 3a) or AAV9-GFP used as controls (not shown).

Accordingly, the expression in skeletal and cardiac muscles after delivery of AAV9-mitoTALEN generated a significant decrease in the mutant/WT mtDNA ratio when compared to a non-targeted tissue such as kidney after 6 and 12 weeks (Fig. 3b,c). When the systemic injection was performed with the control AAV9-GFP, targeted tissues showed no change or increased mutant/WT mtDNA ratios when compared to kidney under the same conditions (Fig. 3b,c).

In addition, we performed intraperitoneal injection in neonate mice (P3), which also resulted in positive expression of the AAV9-mitoTALEN in cardiac and skeletal tissues, with no detectable expression in kidney or brain (Supplementary Fig. 4a). Tissues were analyzed 6 weeks post-injection and lower ratios of mutant/WT mtDNA were observed in heart and gastrocnemious muscle when compared to non-expressing tissues. Because of the mouse-to-mouse variation in heteroplasmy, some of these trends did not reach significance (Supplementary Fig. 4b).

Although most mtDNA molecules are completely degraded after double-strand breaks, at very low frequencies some DNA fragments can form large deletions[12–14]. Testing for the presence of these rare events by long-range PCR failed to detect mtDNA deletions in tibialis anterior of intramuscular-injected mice, heart of systemically injected mice, or transfected C57BL/6J fibroblasts (Supplementary Fig. 5).

MtDNA mutations are major causes of myopathy and cardiomyopathies[15], and for this reason we aimed to treat these tissues in an animal model. Although different mice have different starting levels of mtDNA heteroplasmy, intramuscular expression of mitoTALENs led to reductions in mutant/WT mtDNA ratios in every one of the 21 mice analyzed. Moreover, a single injection of the AAV9-mitoTALEN had a long lasting and stable effect, which probably extended beyond the time of transgene expression. The fact that the

elimination of mutant mtDNA was not complete may actually have benefits. It may avoid rapid mtDNA depletion, which could be dangerous in tissues with extremely high levels of a mutant mtDNA (for example, >95%). The change in heteroplasmy was higher at later time points (that is, 10–24 weeks), probably because the mitoTALEN had more time to cleave the mutant mtDNA.

Although this mouse model has a mild phenotype, the levels of tRNA[Ala] were restored by mitoTALEN treatment, indicating that eliminating a fraction of the mutant mtDNA can effectively correct the molecular mechanism responsible for the disease state.

MtDNA depletion or deletions do not appear to be major side effects of this treatment. Both the partial cleavage of mutant mtDNA and the intrinsic cellular mtDNA copy number control[16] are able to maintain close to normal mtDNA levels. Likewise, increases in mtDNA deletions that can occur after double-strand breaks[12–14] were not detected. It was recently shown that Polg and Mgme1, enzymes of the mtDNA replication complex[17,18], rapidly eliminate broken mtDNA fragments, minimizing the formation of deletions. Moreover, in heteroplasmic cells, the repopulation with the WT genomes probably limits the amplification of low levels of recombinant molecules.

Our results, as well as the ones described in a companion paper by Gammage et al. using mitoZFN[19], show that mitochondrial targeted DNA editing enzymes can be effective in vivo without apparent toxicity. Total elimination of mutant mtDNA may not be necessary, as even small decreases in the mutant mtDNA load can have marked beneficial clinical outcomes[20]. Further studies to deliver effective concentrations of mitoTALENs to other tissues that are commonly involved in mitochondrial diseases will greatly facilitate the implementation of this approach.

Methods

MitoTALEN constructs.

We developed specific mitoTALENs monomers for the tRNA[Ala] m.5024C>T mutation as described in previous publications[3,4]. We designed and constructed plasmids coding for mitoTALEN monomers using the In-Fusion HD cloning kit (Clontech). The final construct included a mitochondrial localization signal derived from SOD2 or modified COX8A/Su9, an immunotag in the N terminus of the mature protein (HA or FLAG), inclusion of a 3′ untranslated region from a mitochondrial gene known to localize mRNA to ribosomes on mitochondria, inclusion of a recoded picornaviral 2A-like sequence (T2A)[10] between the mitoTALEN, and the fluorescent marker for expression (eGFP or mCherry). Obligate heterodimeric *Fok*I domains[8,21] were utilized in all mitoTALENs. The TALEN "A and B" binds the following mtDNA sequences:
*TTGTAAGACTT*catcctacatcTATTGAATGCAAATCAA (sense strand; Tale A binding site in capitals/italics, Tale B binding site is underlined). The TALE-A, 9.5 RVDs, binds to the mutation sequence (m.5024C>T); the TALE-B, 15.5 RVDs, binds to the WT sequence. A shorter version derived from TALE-B was designed, downsizing the number of RVDs from 15.5 to 8.5 (TALE-C). The mitoTALEN was also subcloned into an AAV2 ITR-containing vector (G0347 pFBAAVCMVmcsBgHpA).

Animal model and fibroblasts.

The tRNA[Ala] m.5024C>T mouse model was described by Kauppila et al.[2] at the Max Planck Institute for the Biology of Aging, Cologne, Germany. The mouse carries a pathogenic mutation in the mitochondrial tRNA[Ala] gene and displays disrupted mitochondrial translation caused by instability of the tRNA[Ala][2]. Phenotypes include reduced body mass and age-related cardiomyopathy when high levels of the mutation are present[2]. MEFs derived from the heteroplasmic tRNA[Ala] m.5024C>T mouse were immortalized with the E6-E7 gene from the human papilloma virus[22]. We also used a WT mouse (C57BL/6J) lung fibroblast line.

Cell culture, transfection and sorting.

Heteroplasmic MEFs harboring the tRNA[Ala] point mutation were transfected with GenJet DNA In Vitro Transfection Reagent version II (SL100489; SignaGen Laboratories) as suggested by the manufacturers. After 24 h, cells were sorted using a FACSAria IIU (BD FACSDiva software, Version V8.0.2) by gating on single-cell fluorescence using a 561-nm laser and 600LP, 610/20 filter set for mCherry and a 488-nm laser and 505LP, 530/30 filter set for eGFP. Sorted cells expressing mCherry and eGFP were termed "Yellow"[3,4]. Sorted cells lacking fluorescence were termed "Black".

Generation of a high mutant cell clone derived from the tRNA[Ala] m.5024C>T MEFs using mitoTALEN.

A mitoTALEN was designed to target the WT mtDNA. We used a previously reported mutated version of the TALE N-terminal domain of one of the monomers[23]. The simple substitution of arginine for tryptophan at position 232 results in the alteration of the binding affinity of the TALEN for a typical 5′-T0 to a 5′-G0 position (NT-G)[23]. The re-engineered constructs were made as synthetic DNA fragments (IDT) and cloned using In-Fusion HD (Clontech). The sense strand was targeted by the mitoTALEN monomer (sequence in capital italics) which recognizes a 5′-G0 position (underlined), located two base pairs upstream of the discriminatory base pair "c" (lower case, italics). The monomer binds to the antisense-strand (sequence in lower case) and recognizes the 5′′-T0 (lower case, bold), as follows: 5′-*GAcTGTAAGAC*TTCATCCTACATCTAttgaatgcaaatc**a**-3′ (sense strand). After transfection and single-cell sorting, Clone 5 (85% mutant) was characterized and used for further experiments.

Virus administration and sample preparation.

Recombinant AAV2/9 (here referred to as AAV9) particles were produced by the University of Iowa Viral Core Facility from our designed AAV-mitoTALENs constructs. To achieve intramuscular delivery, adult mice (8–12 weeks old) were injected in the right tibialis anterior, after fur depilation, with $1.0-1.5 \times 10^{12}$ vector genome (vg) of each AAV9-mitoTALENs and the same titer with AAV9-GFP (left tibialis anterior/control leg) (final volume 40 μl in saline). For systemic delivery, mice at P3 were subjected to intraperitoneal or P15/P17 retro-orbital injection with $1.0-1.5 \times 10^{12}$ vg of each AAV9-mitoTALENs in a 40 μl final volume in saline or control AAV-GFP. All injections were carried out using a short insulin syringe with a 31G needle (Becton Dickenson). Tail tissue was obtained at P21

and finger tissue at P3, before performing the injections to determine basal levels of heteroplasmy. At 4, 6, 10, 12, and 24 weeks post-injection, mice were anesthetized and perfused with chilled PBS, and skeletal and cardiac tissues, liver, kidney, brain, and lung samples were obtained. For histological studies, skeletal muscle was embedded in Optimal Cutting Temperature compound (OCT, Fisher Biosciences), fresh-frozen in liquid-nitrogen-cooled isopentane solution and stored at −80 °C. All the procedures with mice were approved by the University of Miami Institutional Animal Care and Use Committee.

Mitochondrial expression of the mitoTALENs.

For western blot studies, 40 μg of total proteins from cellular and tissue homogenates were subjected to electrophoresis in 10% mini-protein stain-free gels (BioRad 456–8034) and transferred to polyvinylidene difluoride membranes using the Trans Blot Turbo system (BioRad 170–4155) according to the manufacturer's instructions. Membranes were developed with SuperSignal West Pico chemiluminescent substrate (34080, Thermo Scientific). The use of TGX Stain-Free Precast Gels allowed the determination of protein loading through gel activation with the imager. Western blots were detected by either Odyssey Infrared Imaging System (LI-COR-Odyssey Version 2.0) or BioRad Chemidoc-Image Lab Version 5.2.1. The antibodies used in western blots were: rat monoclonal antibody to HA (1867423; Roche Biochemical, 1:1,000), mouse monoclonal antibody to FLAG (F3165; Sigma-Aldrich, 1:1,000), mouse monoclonal antibody against GFP (75–131; NeuroMab Antibodies, 1;1,000), mouse monoclonal antibody to Tubulin (T9026, Sigma-Aldrich, 1:1,000), polyclonal antibody against Actin (A2066; Sigma-Aldrich 1:1,000), monoclonal antibody against COXI (ab14705, ABCAM 1:1,000), and monoclonal antibody against NDUFB8 (ab110242, ABCAM, 1:1,000). Secondary antibodies were: IgG, horseradish peroxidase (HRP)-linked antibodies, rat-HRP (A-5795, Sigma-Aldrich, 1:2,000), mouse-HRP (7076, Cell Signaling, 1;2,000), rabbit-HRP (7074, cell Signaling, 1:2,000), goat anti-rat IgG IDylight 680-conjugated (612-144-002, Rockland, 1:5,000), goat anti-rat IgG IDylight 800-conjugated (612-145-002, Rockland, 1:5,000), goat anti-mouse IgG IDylight 680-conjugated (610-144-002, Rockland, 1:5,000), goat anti-mouse IgG IDylight 800-conjugated (610-145-002, Rockland, 1:5,000).

For immunocytochemical studies, HeLa cells were transfected with mitoTALEN plasmids for 24 h, incubated for 30 min at 37 °C with 200 nmol l^{-1} MitoTracker Red CMXRos (M7512, Invitrogen) and fixed with 2% paraformaldehyde for 20 min. Primary antibodies to HA (1:200) or FLAG (1:200) in 2% BSA in phosphate-buffered saline were incubated overnight at 4 °C. The following day, coverslips were incubated for 2 h at room temperature with secondary antibodies: Alexa Fluor 488-conjugated goat antibody to rat IgG (A-11006, Invitrogen, 1:200) or goat antibody to mouse IgG (A-11001, Invitrogen, 1:200) as described[24].

For immunohistochemistry studies, tissue samples were fresh-frozen in isopentane and sectioned using a cryostat (10 μm). After permeabilization and blocking with 0.3% Triton X-100 and 4% goat serum during 30 min in PBS, samples were incubated overnight at 4 °C with a chicken antibody to GFP (Abcam, ab13970, 1:500) and for 2 h at room temperature with secondary goat antibody against chicken (A-11039, Invitrogen, 1:250)[24]. Slides were

mounted with mounting media (Biotium 23004). Images were recorded using a Zeiss LSM510 confocal microscope (software: Fluoview, FV 10-ASW Version 2.00c).

Quantification of m.5024C>T mutation load by "last cycle hot" PCR and RFLP.

We determined the levels of the m.5024C>T mutation by "last-cycle hot" PCR[25] which visualizes only nascent amplicons and removes interference from hetero-duplexes formed during melting and annealing cycles. Total genomic DNA was extracted from FACS sorted cells with the NucleoSpin Tissue XS kit (740901.50; Takara) according to the manufacturer's instructions and from tissues with phenol-chloroform extraction[24]. The DNA concentration was determined spectrophotometrically (BioTek Synergy H1 hybrid). The WT allele for the m.5024C>T mutation completes a mismatched primer, creating a restriction site for *Pst*I not present in the mutant PCR product. The following primers were used: F- 5′-CCACCCTAGCTATCATAAGCACA-3′ and B-5′-AAGCAATTGATTTGCATTCAATAGATGTAGGATGAAGTCCTGCA-3′. PCR products were digested with *Pst*I and resolved in a 12% polyacrylamide gel. The radioactive signal was quantified using a Cyclone phosphor-imaging system (PerkinElmer) and OptiQuant software Version 5.0 (PerkinElmer).

Total mitochondrial DNA levels determination by quantitative PCR.

Quantitative PCR (qPCR) reactions using TaqMan chemistry (PrimeTime Std qPCR Assay, Integrated DNA Technologies) were performed on a Bio-Rad CFX96/C1000 qPCR machine. We used the comparative cycle threshold (Ct) method to determine the relative quantity of mtDNA. The level of mtDNA was determined by quantifying the levels of total mtDNA/ genomic DNA (ND1/18 s or ND5/18 s).

The following primer/probe sets were used:

mtDNA. ND1 = Forward: GCC TGA CCC ATA GCC ATA AT (NC_005089; mtDNA 3282–3301); Reverse: CGG CTG CGT ATT CTA CGT TA (mtDNA 3402–3383).

Probe: /56-FAM/TCT CAA CCC/ZEN/TAG CAG AAA CAA CCG G/3IABkFQ/ (mtDNA 3310–3334).

ND5 = Forward: CCC ATG ACT ACC ATC AGC AAT AG (mtDNA 12432–12454); Reverse: TGG AAT CGG ACC AGT AGG AA (mtDNA 12533–12514).

Probe: /5TET/AGT GCT/ZEN/GAA CTG GTG TAG GGC/3IABkFQ/(mtDNA 12482–12458).

Genomic DNA.—*18 s* = Forward: GCC GCT AGA GGT GAA ATT CT (RefSeq NR_046233.2; chr17:39984253–39984272); Reverse: TCG GAA CTA CGA CGG TAT CT (RefSeq NR_046233.2; chr17:39984432–39984412)

Probe: /5Cy5/AAG ACG GAC CAG AGC GAA AGC AT/3IAbRQSp/ (RefSeq NR_046233.2; chr17:39984285–39984305)

Quantitative PCR reactions using SYBR/ROX chemistry (172–5264; BioRad, SsoAdvanced SYBR Green) employed similar methods and the following

primers: *mtDNA. ND1* = Forward: CAGCCTGACCCATAGCCATA (mtDNA 3280–3299); Reverse: ATTCTCCTTCTGTCAGGTCGAA (mtDNA 3363–3342).

Genomic DNA.—β-Actin = Forward: GCGCAAGTACTCTGTGTGGA (RefSeq NM_007393; chr5: 143665584–143665603); Reverse: CATCGTACTCCTGCTTGCTG (RefSeq NM_007393; chr5:143665515–143665534).

Detection of mtDNA deletions by long-PCR.

To evaluate the possible presence of deletions, DNA was isolated from tibialis anterior muscle after injection at different times (6, 12, and 24 weeks), from heart tissues after retro-orbital injection at 6 and 12 weeks, and from control mouse fibroblasts (C57BL/6J) treated with mitoTALEN after 24 h sorting. Fragments were amplified with a Takara LA Taq Long PCR system (RR002M, Takara Bio) with several primer combinations at 4 min extension times using the following primers: mtDNA nt 3,971F-12,802R; mtDNA primers 5,399F-14,940R at 5 min extension; and primers 14,711F-5,637R at 7 min extension. PCR products were resolved on 0.8% agarose Tris-Acetate-EDTA (TAE) gels. As a positive control we used cortex from a mouse model expressing a mitochondrial-targeted restriction endonuclease (mito*Pst*I) in the brain[26]. This cortex DNA was previously shown to have low levels of *Pst*I-mediated mtDNA deletions (<1%)[26].

RNA isolation and northern blot analysis.

RNA isolation and northern blot analysis was performed according to previous studies[2]. Total RNA was isolated from snap-frozen heart and muscle tissues with TRIzol (Ambion) or the miRNAeasy kit (Qiagen) following the manufacturer's standard protocols. The extracted RNA was resolved on 1.2% formaldehyde-agarose gel followed by a transfer onto Hybond-NX membranes (GE Healthcare). Transcripts of interest were detected with non-radioactive or radioactive methods as previously described[27]. For non-radioactive detection, the membrane was probed with mouse-specific biotin-labeled oligonucleotides by overnight incubation at 50 °C followed by washing and signal detection with IRDye 800CW dye-labeled streptavidin (dilution 1:5,000 in Tris-Borate saline (TBS), 0.05% tween-20) in a LI-COR Biosciences imaging system. For radioactive detection, the Hybond-N + membrane was hybridized with mouse mitochondrial tRNA-specific oligonucleotides labeled with [γ–^{32}P]ATP at 42 °C in PerfectHyb Plus hybridization buffer (Sigma Aldrich) and then washed in 2× and 0.2× SSC/0.1% SDS. Radioactive signals were detected by autoradiography and quantified using a phosphorimager imaging system (Fuji FLA 7000).

Statistical analysis.

Data analysis was performed using GraphPad Prism 7 and presented as mean ± s.d. Pairwise comparisons were performed using two-tailed unpaired Student's *t*-test assuming equal variance. A *P* value of <0.05 was considered significant.

Original blots.

Uncropped blots are shown in Supplementary Figs. 6, 7, and 8.

Ethical compliance.

We declare compliance with all relevant ethical regulations.

Reporting Summary.

Further information on research design is available in the Nature Research Reporting Summary linked to this article.

Data availability

All the data contained in this manuscript is available to investigators.

Supplementary Material

Refer to Web version on PubMed Central for supplementary material.

Acknowledgements

References

1. Craven L, Alston CL, Taylor RW & Turnbull DM Recent advances in mitochondrial disease. Annu. Rev. Genomics Hum. Genet 18, 257–275 (2017). [PubMed: 28415858]

2. Kauppila JH et al. A phenotype-driven approach to generate mouse models with pathogenic mtDNA mutations causing mitochondrial disease. Cell Rep 16, 2980–2990 (2016). [PubMed: 27626666]

3. Bacman SR, Williams SL, Pinto M, Peralta S & Moraes CT Specific elimination of mutant mitochondrial genomes in patient-derived cells by mitoTALENs. Nat. Med 19, 1111–1113 (2013). [PubMed: 23913125]

4. Hashimoto M et al. MitoTALEN: a general approach to reduce mutant mtDNA Loads and restore oxidative phosphorylation function in mitochondrial diseases. Mol. Ther 23, 1592–1599 (2015). [PubMed: 26159306]

5. Gammage PA et al. Near-complete elimination of mutant mtDNA by iterative or dynamic dose-controlled treatment with mtZFNs. Nucleic Acids Res 44, 7804–7816 (2016). [PubMed: 27466392]

6. Lehmann D et al. Pathogenic mitochondrial mt-tRNA(Ala) variants are uniquely associated with isolated myopathy. Eur. J. Hum. Genet 23, 1735–1738 (2015). [PubMed: 25873012]

7. Cermak T et al. Efficient design and assembly of custom TALEN and other TAL effector-based constructs for DNA targeting. Nucleic Acids Res 39, e82 (2011). [PubMed: 21493687]

8. Miller JC et al. An improved zinc-finger nuclease architecture for highly specific genome editing. Nat. Biotechnol 25, 778–785 (2007). [PubMed: 17603475]

9. Li T et al. TAL nucleases (TALNs): hybrid proteins composed of TAL effectors and FokI DNA-cleavage domain. Nucleic Acids Res 39, 359–372 (2011). [PubMed: 20699274]

10. Szymczak AL et al. Correction of multi-gene deficiency in vivo using a single 'self-cleaving' 2A peptide-based retroviral vector. Nat. Biotechnol 22, 589–594 (2004). [PubMed: 15064769]

Author Manuscript   Author Manuscript   Author Manuscript   Author Manuscript

11. Yardeni T, Eckhaus M, Morris HD, Huizing M & Hoogstraten-Miller S Retro-orbital injections in mice. Lab. Anim. (NY) 40, 155–160 (2011). [PubMed: 21508954]

12. Srivastava S & Moraes CT Double-strand breaks of mouse muscle mtDNA promote large deletions similar to multiple mtDNA deletions in humans. Hum. Mol. Genet 14, 893–902 (2005). [PubMed: 15703189]

13. Fukui H & Moraes CT Mechanisms of formation and accumulation of mitochondrial DNA deletions in aging neurons. Hum. Mol. Genet 18, 1028–1036 (2009). [PubMed: 19095717]

14. Bacman SR, Williams SL & Moraes CT Intra- and inter-molecular recombination of mitochondrial DNA after in vivo induction of multiple double-strand breaks. Nucleic Acids Res 37, 4218–4226 (2009). [PubMed: 19435881]

15. El-Hattab AW & Scaglia F Mitochondrial cardiomyopathies. Front. Cardiovasc. Med 3, 25 (2016). [PubMed: 27504452]

16. Kelly RD, Mahmud A, McKenzie M, Trounce IA & St John JC Mitochondrial DNA copy number is regulated in a tissue specific manner by DNA methylation of the nuclear-encoded DNA polymerase gamma A. Nucleic Acids Res 40, 10124–10138 (2012). [PubMed: 22941637]

17. Nissanka N, Bacman SR, Plastini MJ & Moraes CT The mitochondrial DNA polymerase gamma degrades linear DNA fragments precluding the formation of deletions. Nat. Commun 9, 2491 (2018). [PubMed: 29950568]

18. Peeva V et al. Linear mitochondrial DNA is rapidly degraded by components of the replication machinery. Nat. Commun 9, 1727 (2018). [PubMed: 29712893]

19. Gammage PA et al. Genome editing in mitochondria corrects a pathogenic mtDNA mutation in vivo. Nat. Med 10.1038/s41591-018-0165-9 (2018).

20. Petruzzella V et al. Extremely high levels of mutant mtDNAs co-localize with cytochrome c oxidase-negative ragged-red fibers in patients harboring a point mutation at nt 3243. Hum. Mol. Genet 3, 449–454 (1994). [PubMed: 7912129]

21. Doyon Y et al. Enhancing zinc-finger-nuclease activity with improved obligate heterodimeric architectures. Nat. Methods 8, 74–79 (2011). [PubMed: 21131970]

22. Lochmuller H, Johns T & Shoubridge EA Expression of the E6 and E7 genes of human papillomavirus (HPV16) extends the life span of human myoblasts. Exp. Cell Res 248, 186–193 (1999). [PubMed: 10094825]

23. Lamb BM, Mercer AC & Barbas CF 3rd Directed evolution of the TALE N-terminal domain for recognition of all 5' bases. Nucleic Acids Res 41, 9779–9785 (2013). [PubMed: 23980031]

24. Bacman SR, Williams SL, Garcia S & Moraes CT Organ-specific shifts in mtDNA heteroplasmy following systemic delivery of a mitochondria-targeted restriction endonuclease. Gene Ther. 17, 713–720 (2010). [PubMed: 20220783]

25. Moraes CT, Ricci E, Bonilla E, DiMauro S & Schon EA The mitochondrial tRNA(Leu(UUR)) mutation in mitochondrial encephalomyopathy, lactic acidosis, and strokelike episodes (MELAS): genetic, biochemical, and morphological correlations in skeletal muscle. Am. J. Hum. Genet 50, 934–949 (1992). [PubMed: 1315123]

26. Pinto M, Nissanka N & Moraes CT Lack of parkin anticipates the phenotype and affects mitochondrial morphology and mtDNA levels in a mouse model of Parkinson's disease. J. Neurosci 38, 1042–1053 (2018). [PubMed: 29222404]

27. Davies SM et al. MRPS27 is a pentatricopeptide repeat domain protein required for the translation of mitochondrially encoded proteins. FEBS Lett 586, 3555–3561 (2012). [PubMed: 22841715]
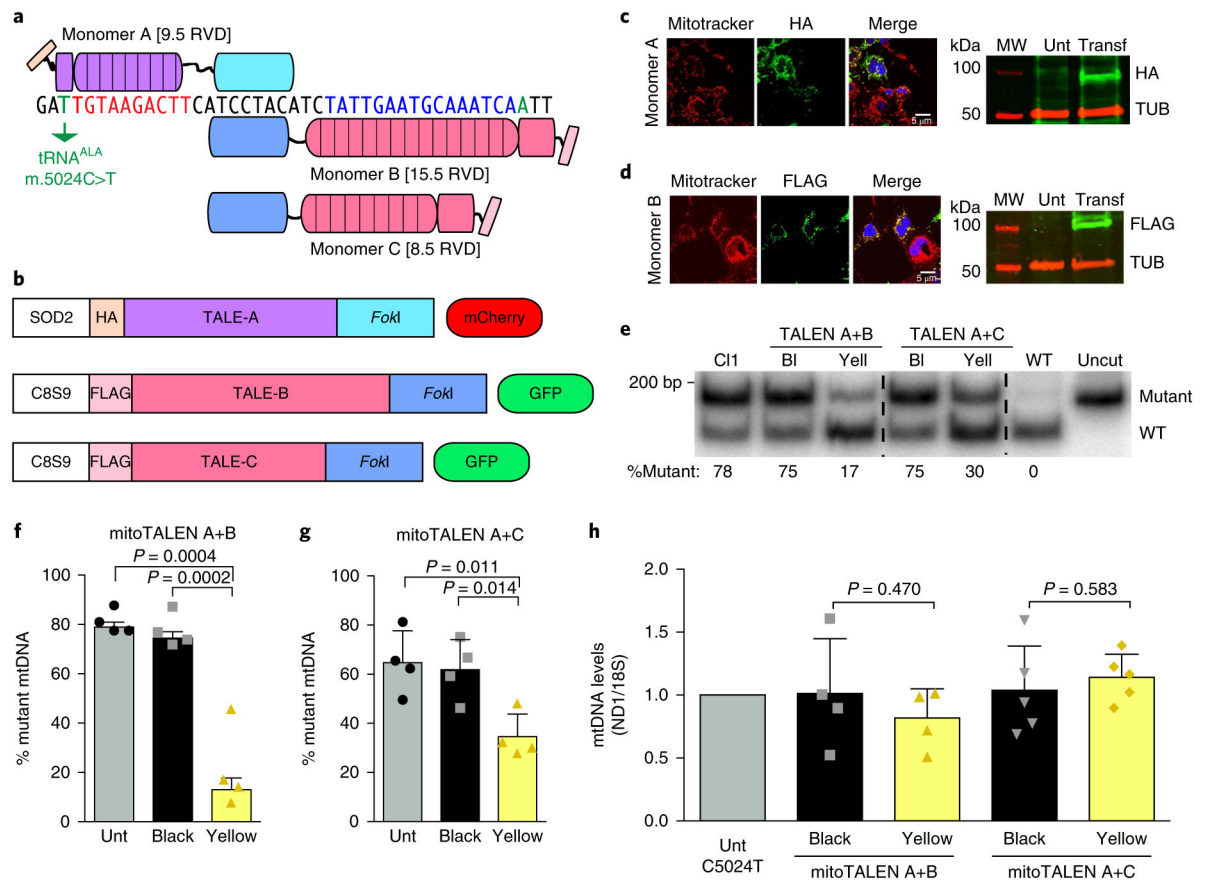
Fig. 1 |. Development of a mitoTALEN for the mouse mutant m.5024C>T mtDNA.
a,b, Structure of mitoTALEN monomers, which include: (i) a basic TAL-binding domain[7]; (ii) a mitochondrial localization signal in the N terminus (Cox8-Sub9 or SOD2); (iii) a unique tag (HA or FLAG) for immunological detection; (iv) a GFP or mCherry separated from the mitoTALEN by a picornaviral 2A-like sequence (T2A)[10] for sorting of transfected cells; (v) a 3′UTR untranslated region from a nuclear gene (ATP5B or SOD2 mRNA); (vi) *Fok*I that works as a heterodimer (NEL only dimerizes with CKK). Panel **a** also shows the binding site of the monomers to the mtDNA. The mutation is at position T0 (arrow). **c,d**, Tag detection in HeLa cells transfected with mitoTALEN monomers. Mitochondrial localization was determined with Mitotracker Red (left panels) and protein size by western blots (right panels). Scale bar, 5μm. Monomer A, 9.5 RVDs, 84.2 kDa; monomer B, 15.5 RVDs, 112,5 kDa. Experiments were performed twice with similar results. MW, molecular weight markers; Unt, untransfected cells; Transf, transfected cells; TUB, tubulin. **e**, MtDNA analyses of transfected heteroplasmic MEFs after sorting. Cells were sorted for the fluorescent markers 24 h after transfection and analyzed by PCR/RFLP to differentiate the mutant from the WT mtDNA. WT refers to DNA from a WT C57BL/6J mouse. Experiments were repeated four times with similar results. Cl1, clone 1; Bl, sorted "black" population; Yell, sorted "yellow" population. **f,g**, Quantification of heteroplasmy, using mitoTALEN A + B (mean ± s.d.; $n = 4$ independent experiments) or the mitoTALEN A + C (mean ± s.d.; $n = 4$ independent experiments). **h**, MtDNA depletion (ND1 mtDNA gene/18S nuclear gene)

was not observed after sorting (24h) (mean ± s.d.; $n = 4$ independent experiments). Statistics done by two-tail Student's t-test.
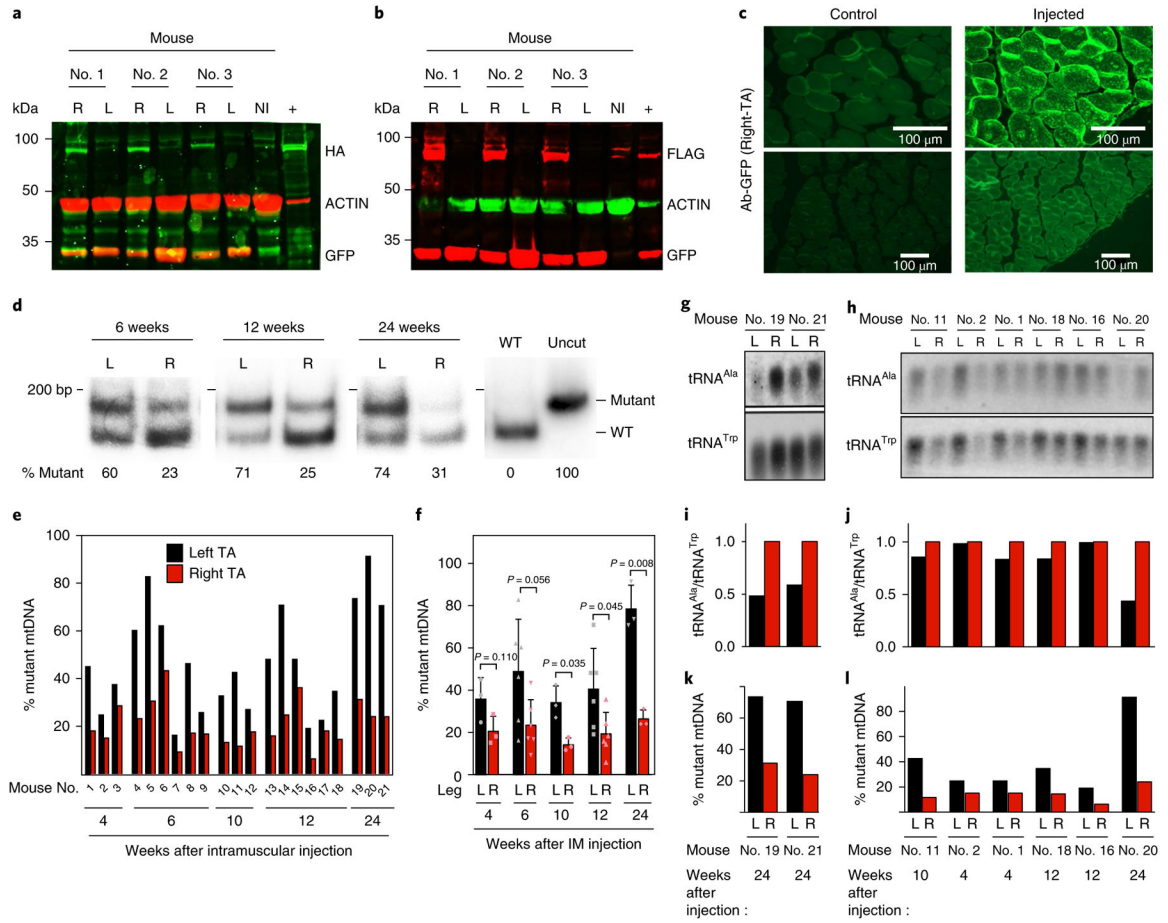
Fig. 2 |. AAV9-MitoTALEN is expressed in skeletal muscle and shifts mtDNA heteroplasmy in a predicted manner.
a,b, Western blots showing expression of mitoTALENs in the right (R) and GFP in the left(L) tibialis anterior 4 weeks after recombinant AAV9 intramuscular injections. HA (**a**), FLAG (**b**), and GFP (**a,b**). (+): positive controls are homogenates of HeLa cells transiently transfected with each monomer. NI represents non-injected tibialis anterior muscle. These experiments were repeated for every injected tibialis anterior. **c**, Immunocytochemistry analysis showed positive GFP expression in the right tibialis anterior (24 weeks post-injection). These experiments were performed twice with similar results. Scale bar, 100μm. **d**, Representative PCR/RFLP showing a decrease in the mutant mtDNA 4–24 weeks after injection. **e**, Percentage of mutant mtDNA in left and right tibialis anterior in each mouse. **f**, Averages of "time groups" from panel **e** (4 week, $n = 3$; 6 weeks, $n = 6$; 10 weeks, $n = 3$; 12 weeks, $n = 6$; 24 weeks, $n = 3$). Statistics done by two-tail Student's t-test. **g–j**, High-resolution northern blots showing the tRNA^{Ala} and RNA^{Trp} levels in the left and right tibialis anterior of two mice after 24 weeks post-injection (**g,i**) and six additional mice after 4, 10, 12, and 24 weeks post-injection (**h,j**). These experiments were repeated twice with similar results. **k,l**, The percentage of mutant mtDNA change from the right tibialis anterior (injected with AAV9-mitoTALEN) to the left (injected with AAV9-GFP) is also shown for the same mice analyzed for tRNAs levels (data extracted from panel **e**).
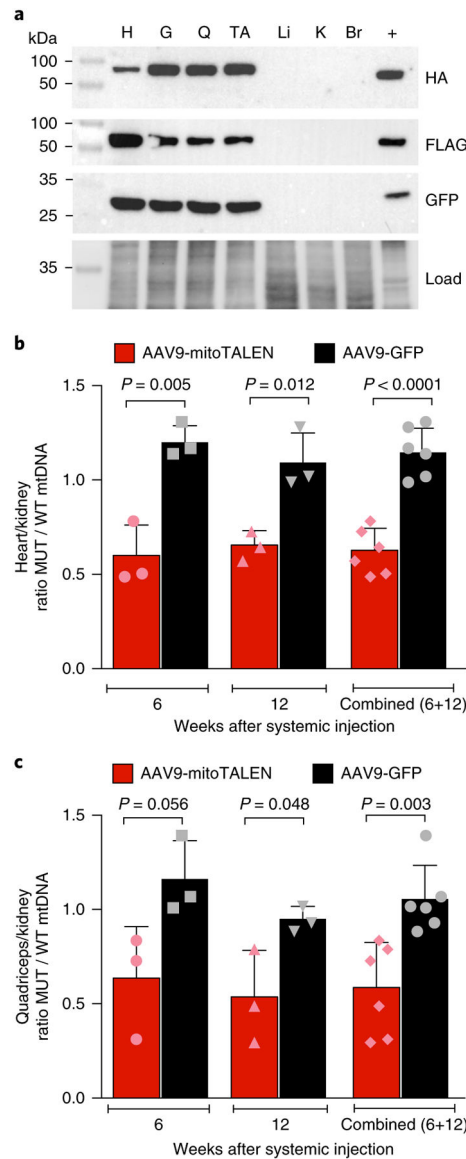
Fig. 3 |. AAV9-mitoTALENs induce a significant and persistent shift in mtDNA heteroplasmy in heart and skeletal muscle after systemic injection.
a, Expression of mitoTALEN (western blot for FLAG, HA and GFP) observed in heart and skeletal muscle after 6 weeks. Tissues analyzed: heart (H), gastrocnemius (G), quadriceps (Q), tibialis anterior (TA), liver (Li), kidney (K), and brain (Br). (+): positive controls are homogenates of HeLa cells transiently transfected with each monomer. Load equalis total proteins in membrane. These experiments were performed three times with similar results.
b,c, Quantification of the mutant/wild-type (MUT/WT) mtDNA load in heart (**b**) and quadriceps (**c**) normalized to kidney, a tissue not targeted by AAV9, after 6 and 12 weeks post systemic delivery of the AAV9-mitoTALENs and AAV9-GFP (mean ± s.d.; 6 week, $n = 3$; 12 weeks, $n = 3$; combined, $n = 6$).